Ain Shams Engineering Journal 14 (2023) 102061

Contents lists available at ScienceDirect

Ain Shams Engineering Journal

journal homepage: www.sciencedirect.com

Design and analysis of PV fed high-voltage gain DC-DC converter using PI and NN controllers

Madisa V.G. Varaprasad [a], N.S.S. Ramakrishna [d], Innocent Kamwa [c,*], M. Venkatesan [b], Dasari Manikanta Swamy [d], S.M. Muyeen [e], Sk. A. Shezan [f,g], Md. Fatin Ishraque [h]

[a] Department of Electrical and Electronics Engineering, Vignan's Institute of Information Technology, Duvvada, Visakhapatnam 530049, India
[b] Department of Electrical and Electronics Engineering, Vignan's Lara Institute of Technology and Science, Vadlamudi, Guntur 522213, India
[c] Department of Electrical Engineering and Computer Engineering, Laval University, Canada
[d] Department of Electrical and Electronics Engineering, GMRIT, RAJAM, India
[e] Department of Electrical Engineering, Qatar University, Doha 2713, Qatar
[f] Department of Electrical Engineering, Engineering Institute of Technology, Melbourne Campus, Melbourne, VIC 3001, Australia
[g] Department of Electrical and Electronics Engineering, Green University of Bangladesh, Bangladesh
[h] Department of Electrical and Electronics Engineering, Pabna University of Science and Technology, Pabna, Bangladesh

ARTICLE INFO

Article history:
Received 14 May 2022
Revised 29 October 2022
Accepted 18 November 2022
Available online 12 December 2022

Keywords:
CI
PI
NN
Passive clamp circuit
DC-DC converter

ABSTRACT

The entire globe is now focused on generating power using solar photovoltaic (SPV) cells. The SPV is generating the DC power, by using power converters to satisfy the load requirement. In this article, a modified High-Voltage DC-DC converter was explained. The main intention of the modified converter is to decrease the reverse recovery currents and voltage stress across the switch, similarly, it generates high voltage at the converter output. The modified converter contains mainly-one diode, two capacitors, and Coupled Inductor (CI). When the converter switch comes under active state two capacitors are discharged in series, similarly when the converter switch under inactive state those two capacitors are charged in parallel through the coupled inductor (CI) energy so, to get a high voltage at the converter output side. To reuse the leakage-inductor (LI) energy of the CI with the help of a passive clamp circuit for reducing the voltage stress across the switch, similarly switch has less resistance so conduction losses also decreased. In this manner, the converter efficiency was improved and the diode recovery problem also solved. For the converter duty cycle controlling, Proportional-Integral (PI) and Neural Network (NN) controllers were used. The performance and analysis of the modified converter were described in detail with the help of both controllers. Here, 48 V is doubled to 400 V. By modifying the converter's parameters, its behavior is evaluated. In this converter, voltage spikes and reverse recovery currents should be minimal. The converter's switching pulse can be adjusted by PI or NN. The entire system was designed in MATLAB/ Simulink tool.

1. Introduction

The world's population is growing at an increasing rate, and electricity demand has risen in response to their greater quality of living [1]. Electric power plays a key role in enabling people to live their lives, and as a result, all countries are looking forward to generating electricity from a variety of sources, including coal, oil, and renewable energy sources [2]. Many renewable energy sources, such as hydro, tidal, wind, and solar, are now used to generate electricity [3]. Solar-based electric power generation is the most concentrated of these since it is pollution-free, has a low cost, and has a large energy potential for electrical power generation [4]. According to an assessment on the renewable energy system, India plans to create 175 GW of renewable energy by 2022, with wind and solar providing 90 % of the energy [5]. Solar energy has grown at a quick rate of 20–25 percent in India during the previous several years. Solar cell efficiency is quickly increasing, and manufac-

* Corresponding author.
E-mail address: innocent.kamwa@gel.ulaval.ca (I. Kamwa).
Peer review under responsibility of Ain Shams University.

Production and hosting by Elsevier

https://doi.org/10.1016/j.asej.2022.102061
2090-4479/

turing processes are also improving, which is a major contributor in cost reduction. The design of the PV cell has been thoroughly addressed using mathematical formulas. Using MPPT (Maximum Power Point Tracking) controllers to get the most power out of the PV [6]. Temperature and irradiation are important factors in achieving maximum PV power [7].

Basically, the PV cells generate low output power, for generating a high output power the PV cells are arranged in series connection [8]. In this case, the shadow effect will come so it's not a good solution for generating high output power [9]. Then connect the boost converter to the PV cells to generate a huge voltage. The conventional boost converter produces high voltage with more duty cycle but in the experimental, the standard boost converter unable to generate a high-voltage at the output side due to reverse recovery issue [10]. Because of this problem, the overall efficiency of the system is decreased and electromagnetic interference (EMI) problem also occurs [11–12]. For improving high-voltage and efficiency so many step-up converter topologies are examined so far [13]. Few converters, fly back and forward converters are can regulate the transformer turns ratio to get high-voltage [14].

Due to the LI of the transformer, the converter switch faces power dissipation and voltage spike problems even yet the active clamp and non-dissipative snubber circuit was taken, the price is also increased because of the extra power switches [15]. By using voltage lift and switched capacitor methods to get a high-voltage [16]. Still, switch face some problems like conduction loss and high charging current. By using the CI in the converter to get high-voltage. But the LI produces the voltage spikes across the switch and influence the efficiency of the system [17]. For this cause, the CI along with an active clamp circuit was used in the converter [18]. Likewise, the LI energy is straight reused to the load, to minimize the voltage spike across the converter switch [19]. Moreover, to vary the CI turns ratio to adjust the voltage stress across the converter switch. To attain a high-voltage, it has been suggested that forward and flyback converters are utilized in the secondary side of the CI [20].

Similarly, so many authors proposed to combine a converters output-voltage to rise the voltage gain [21]. Moreover, use more than one CI in the converter to get high-voltage. So, to attain high-voltage and better efficiency, this article proposed a modern clamp-mode and high step-up converter [22–23]. The modified converter has two diodes and two capacitors on the secondary side of the CI. Those two capacitors are discharged in series and charged in parallel through the CI, still, high-voltage spikes and power loss are present across the switch because of leakage inductor of the CI. Thus, LI energy is reused and the voltage level of the switch is clamped by using a clamping circuit. Finally, one more diode is added on the front side of the converter it protects the system in case of reverse direction of current flow in the circuit by using PI and NN controllers to control the switching pulse of the converter. The converters were connected to the generated PV arrays' 3-phase RL load. The non-linear power boost converter, PV module, and inverter make up the system. The system is strong and dependable thanks to the suggested PWM control method[26]. DC-DC converters are a type of power electronic equipment that is particularly useful for regulating DC voltage and increasing the efficiency of renewable energy sources.The total efficiency and effectiveness of power grids are greatly influenced by the care with which the DC-DC converter is chosen. In addition to picking a reliable DC-DC conversion method, it's crucial to incorporate an appropriate control strategy for the best possible performance [27].

The performance and analysis of the modified High-Voltage DC-DC converter were explained in detail with the help of both controllers. The entire system was designed in MATLAB/ Simulink tool.

Comparison of Non-Isolated DC-DC Converter Topologies.

Converter	Features	Advantages Limitations	Limitations
Buck Boost Converter	Lowcomplexity Cost effectiv	Suitable for low power applications	Voltage imbalance for multi-input and multi-output application
High Step-Up DC-DC Converter	Mediumcomplexity Moderate cost	Non-inverting output Utilized for renewable energy applications	Suitable for multi-input single-output configuration Input conduction losses due to coupled inductors
High Gain Input-Parallel Output-Series DC-DC	Mediumcomplexity Moderate cost	Non-inverting output Less reverse recovery period and low output ripples	Unidirectional power flow Transient issues due to diode reverse recovery issue and charging of capacitors

2. Modified high-voltage dc-dc converter

The modified High-voltage DC-DC converter has 48 V DC input voltage (V_{in}), one coupled inductor (CI), the CI has N_s and N_p, one main switch (S), output capacitor (C_0), output diode (D_0), clamp capacitor (C_1), clamp diode (D1), two diodes (D2 and D3) and two capacitors (C_2 and C_3). The CI has leakage inductor (LI) L_k, magnetizing inductor (MI) L_m and an ideal transformer. Fig. 1 (a) signifies the block diagram of the proposed converter and Fig. 1(b) signifies the circuit diagram of the High-Voltage DC-DC converter.

The energy in the LI of the CI is reused to C_1, and the switch voltage also clamped. The voltage stress across the switch is decreased randomly because the switch has less resistance. The innovative voltage-clamp topology was primarily projected in [23] to recover the energy in the LI. The modified converter has an association with the CI and switched-capacitor methods. The concept of the switch capacitor method has been suggested in [2]. So, when the switch is an active state those two capacitors are discharged in series similarly when the switch is an inactive state those two capacitors are charged in parallel through the CI. By tuning the CI turns ratio, the voltage around the capacitors can be controlled then high-voltage can be attained. Therefore, the modified converter has less conduction loss and reduces the reverse-recovery problem of the diodes. The modified DC-DC converter works on both Continuous Conduction Stage (CCS) and Discontinuous Conduction Stage (DCS).

The different stages of CCS and the working, mathematical analysis and operating stages of the modified converter are described below. Fig. 2 represents the operating stages of the modified converter in CCS. To assume the following conditions the circuit analysis is very easy, 1) all capacitors are considered large enough. 2) The CI coupling coefficient is$K = \frac{L_m}{(L_m+L_k)}$. 3) Similarly, CI turns ratio n = Ns/NP. Fig. 3 represents the characteristics of the modified converter in CCS.

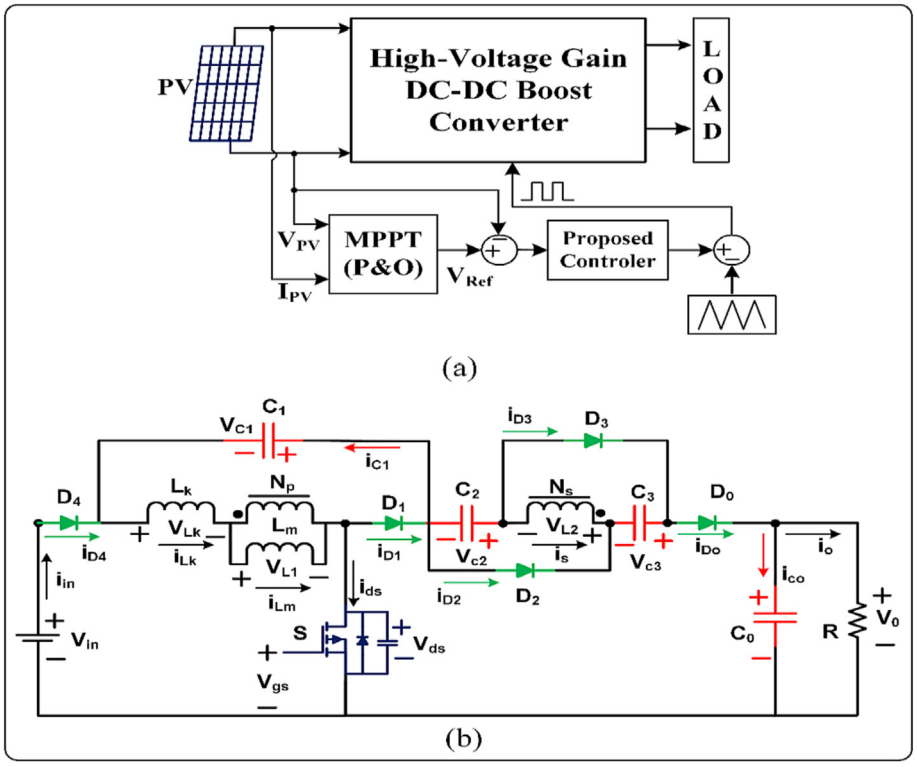

Fig. 1. Circuit diagram of the modified Converter.

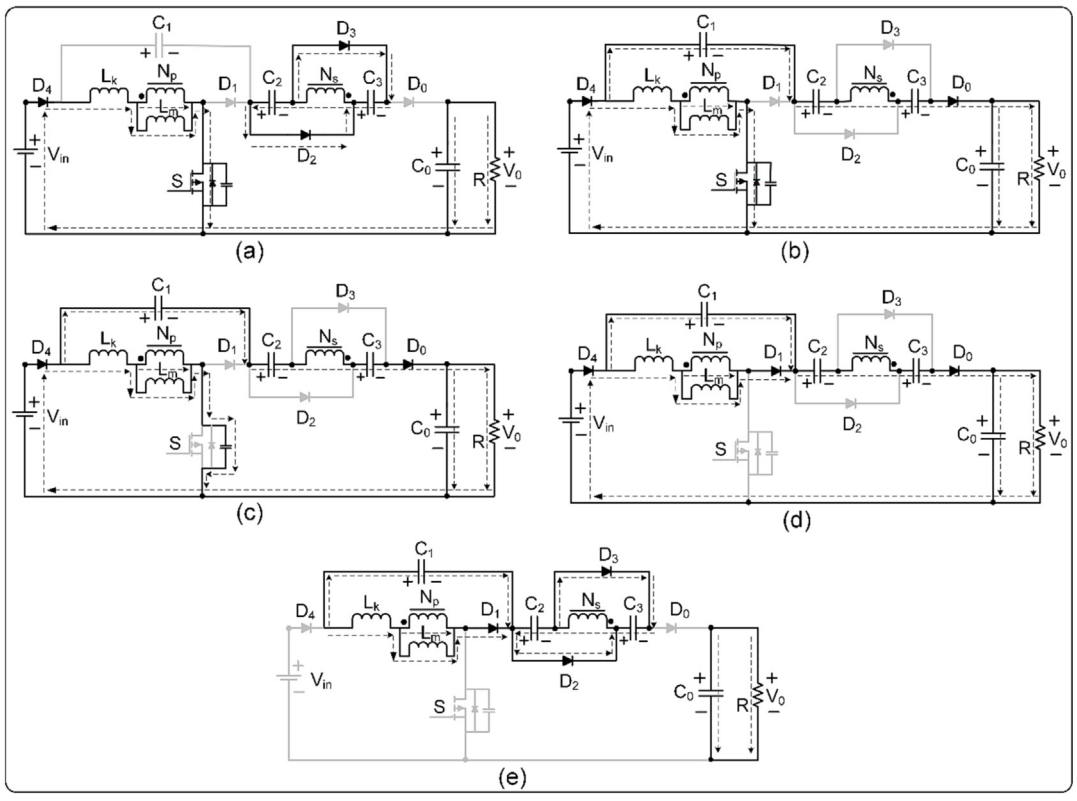

Fig. 2. States of operation of modified converter in CCS.

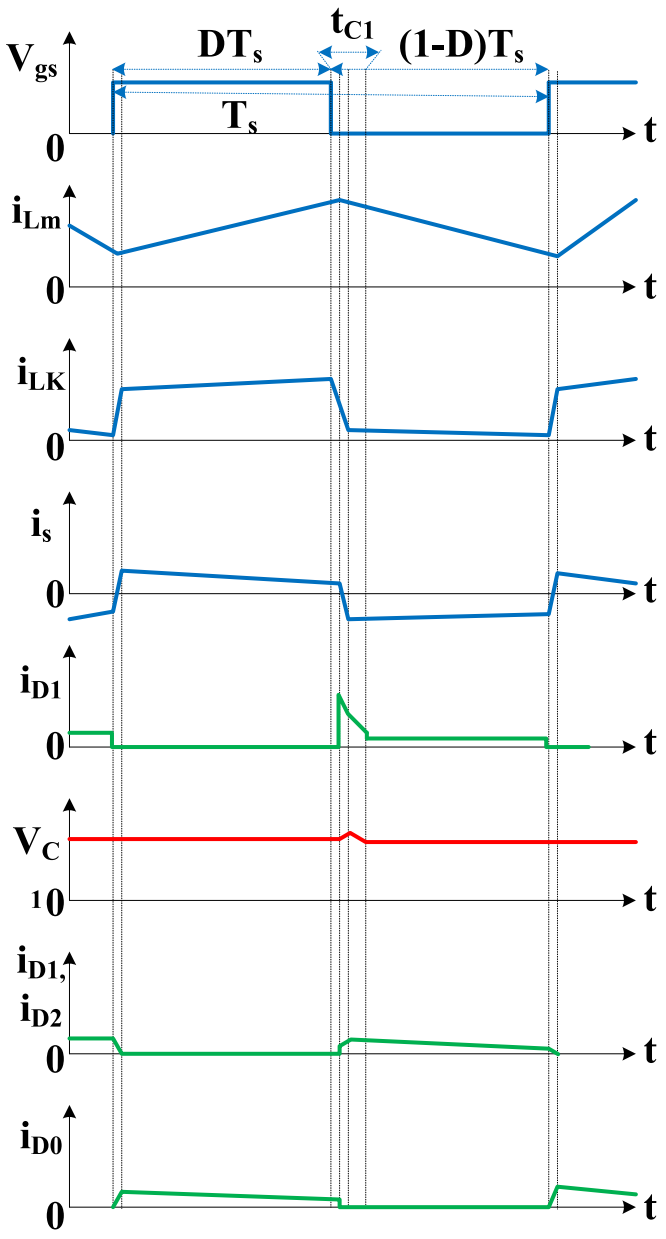

Fig. 3. The characteristic waveform for CCS.

2.1. CCS operation

The different stages of CSS are shown in Fig. 2.

Stage I: The diodes, D_O and D_1 are in the inactive state, and D_2 and D_3 are in the active state. In this stage, the switch is closed. The voltage expression on the magnetic and leakage inductors is

$$V_{in} = V_{Lk} + V_{Lm}$$

V_{in} charges the L_k, CI current i_s of the secondary side is reduced linearly due to leakage inductor L_k. The C_O delivers its energy to the R. At t = t1 current $i_{D2} = 0$, then stage one ends. Fig. 2. represents the stage I operation of the converter in CCS.

Stage II: In stage two, D_1, D_2, and D_3 are in the inactive state, and D_0 is in the active state. In this stage, the switch is closed. The input voltage V_{in}charges the energy to the MI (L_m) as well as transfers some energy to the secondary side via a CI. The produced voltage is discharged through the C_0 and R. If S is open, Stage II is terminated at t = t_2. Fig. 2. represents the stage II operation of the converter in CCS.

Stage III: In stage three D_1, D_2, and D_3 are in the inactive state, and D_0 is in the active state. In this interval, the switch is open. The main switch of the parasitic capacitor (C_{ds}) is charged via MI (L_m) and LI (L_k). The C_o is delivering its energy to R. D_1 conducts when the voltage of the capacitor $V_{C1} = V_{in} + V_{ds}$, at t = t_3, stage III is terminated. Fig. 2. represents the stage III operation of the converter in CCS.

Stage IV: In stage four D_1 and D_0 are in the active states, and D_2 and D_3 are in the inactive state. In this interval, the switch is open. The clamp capacitor C_1 is charged through the LI (L_m) and MI (L_m), later LI (L_k) energy is recycled. The CI voltage V_{L2} is charging C_0 as well as R, till the i_s equal to zero. In the meantime, D_2 and D_3 start to an active state. If $i_{D0} = 0$, at t = t_4, stage IV is terminated. Fig. 2. represents the stage IV operation of the converter in CCS.

Stage V: In stage five D_1, D_2, and D_3 are in the active state and D_0 is in the inactive state. In this stage, the switch is closed. Output capacitor C_0 is discharged through the R. The C_1 is charged by the MI (L_m) and LI (L_k). The MI (L_m) is released through the second end of the CI and charges the C_2 and C_3. Therefore, C_2 and C_3 are parallel charged. LI (L_k) energy charge C_1, the current i_{Lk} reduces and rises gradually. At, t = t_6, stage V is terminated. Fig. 2. represents the stage V operation of the converter in CCS. Fig. 3 indicates the column diagram for duty ratio versus output voltage of the modified converter.

2.2. DCS operation

By neglecting LI (L_k) of the CI, the steady of DCS is made easy. In the DCS section mainly-three Stages are described.

Stage-I: In stage one D_1, D_2, and D_3 are in the inactive state, and D_O is in the active state. In this stage, the switch is closed. DC source (V_{in}) transfers the energy to the MI (L_m) Thus, MI current (i_{LM}) rises linearly. Also, V_{in} transfers the energy to the secondary side via CI, then capacitors are connected in series the energy is transferred to the C_O and R. When S is open, stage I is terminated at, t = t_1. Fig. 4. represents the stage I operation of the converter in DCS.

Stage-II: In stage two D_1, D_2, and D_3 are in the active state and D_0 is in the inactive state. In this period S is open. The C_1, C_2, and C_3 are charged through the MI (L_m). The C_O is delivering its energy to the R. Stage 2 is terminated when MI (L_m) energy is exhausted at, t = t_2. Fig. 4. represents the stage II operation of the converter in CCS.

Stage-III: In stage three the switch remains open. MI (L_m) energy is exhausted, the C_O energy is discharged through the R. When the switch is closed then Stage three is terminated. Fig. 4 represents the stage III operation of the converter in DCS. Fig. 5 represents the characteristic waveform of the converter in DCS.

3. Modelling and anayltic analysis of the modified converter

3.1. Continuous conduction stage

Let, L_k has released energy to the capacitor the duty cycle D_{C1} is

$$D_{C1} = \frac{t_{C1}}{T_S} = \frac{2(1-D)}{n+1} \tag{1}$$

Where t_{c1} = Time interval

$$V_{Lk}^2 = \frac{L_{k1}}{L_m + L_{k1}} V_{in} = (1-k)V_{in} \tag{2}$$

$$V_{L1}^2 = \frac{L_m}{L_m + L_{k1}} V_{in} = kV_{in} \tag{3}$$

$$V_{L2}^2 = nV_{L1}^2 = nkV_{in} \tag{4}$$

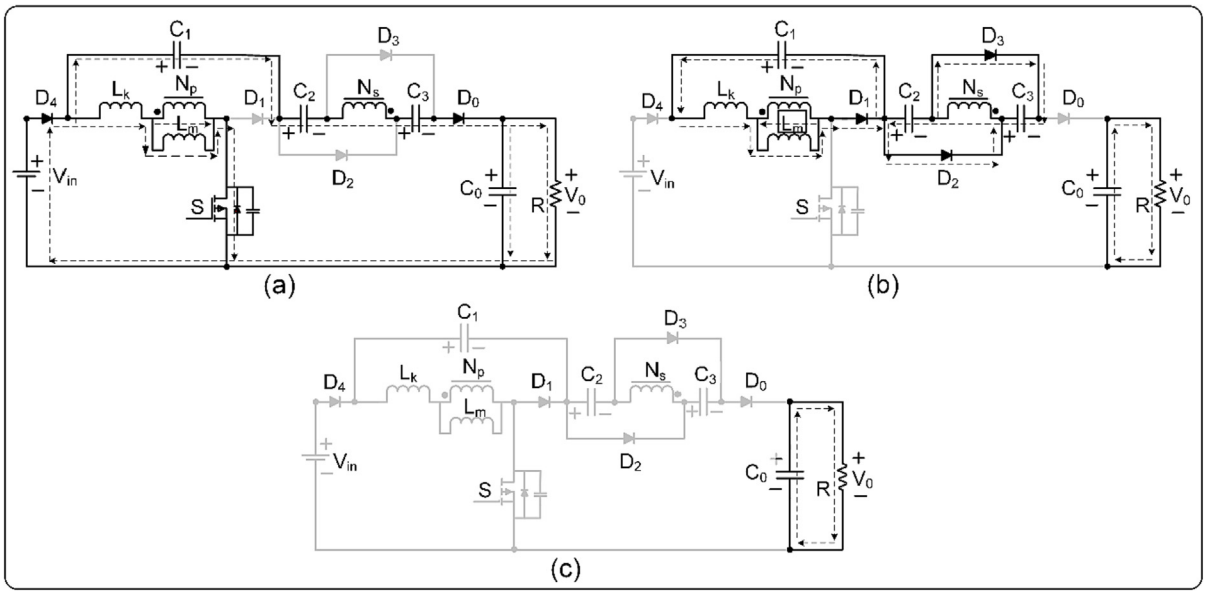

Fig. 4. States of operation for the modified converter in DCS.

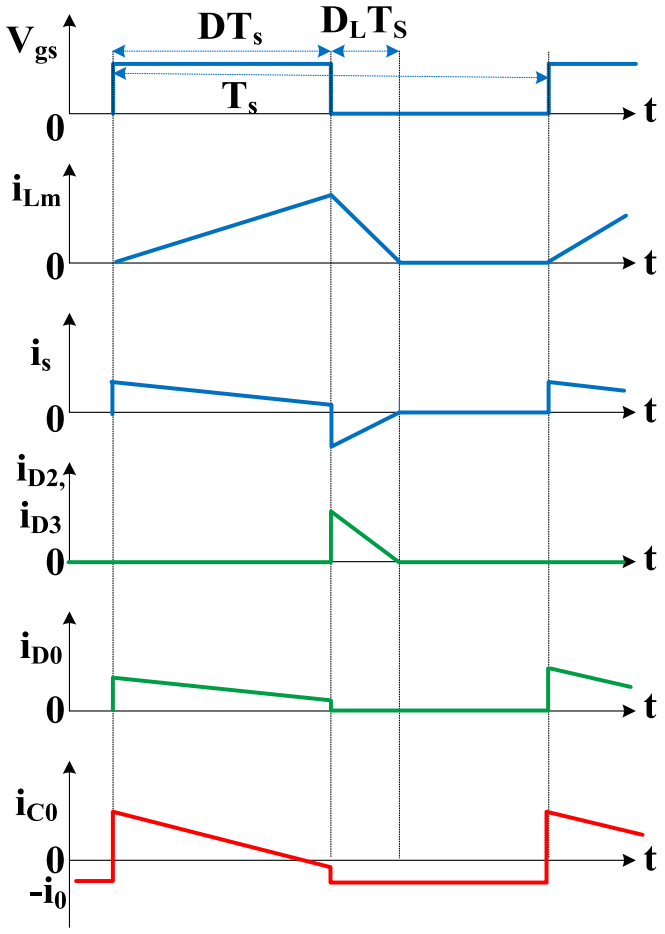

Fig. 5. Characteristic waveforms for DCS.

$$V_0 = V_{in} + V_{C1} + V_{C2} + V_{L2}^2 + V_{C3} \tag{5}$$

The principle of voltage second balance is

$$\int_0^{DT_S} V_{Lk}^2 dt + \int_{DT_S}^{T_S} V_{Lk}^5 dt = 0 \tag{6}$$

$$\int_0^{DT_S} V_{L1}^2 dt + \int_{DT_S}^{T_S} V_{L1}^5 dt = 0 \int_0^{DT_S} V_{L2}^2 dt + \int_{DT_S}^{T_S} V_{L2}^5 dt = 0 \tag{8}$$

Substituting equations (1) to (4) into equations (6) to (8).

$$V_{Lk}^5 = -\frac{D(n+1)(1-k)}{2(1-D)} V_{in} V_{L1}^5 = -\frac{Dk}{1-D} V_{in} V_{L2}^5$$

$$= -\frac{nDk}{1-D} V_{in} \tag{11}$$

The capacitor voltages are

$$V_{C1} = -V_{Lk}^5 - V_{L1}^5 \tag{12}$$

$$= \frac{D}{1-D} V_{in} \frac{(1+k)+(1-k)n}{2}$$

$$V_{C2} = V_{C3} = -V_{L2}^5 = \frac{nDk}{1-D} V_{in} \tag{13}$$

Finally the voltage-gain of the converter is $M_{CCS} = \frac{V_0}{V_{in}} = \frac{1+nk}{1-D} + \frac{D}{1-D} \frac{(k-1)+n(1+k)}{2}$ (14).

Fig. 6 indicates the column diagram for duty ratio versus output voltage of the modified converter. Table. 1 indicates the output voltage of the converter with a varying duty ratio from 0.1 to 0.9.

In Table 2 represents the duty ratio versus voltage gain under n = 3 and varying k values, the k (coupling coefficient) values are taken 1.0, 0.98, and 0.95. If the duty ratio is 0.9 with a k value of 1.0 the converter produces 67 V, If the duty ratio is 0.9 with a k value of 0.98 the converter produces 66.04 V, If the duty ratio is 0.9 with a k value of 0.95 the converter produces 64.4 V, from table 2 we can observe by changing the k value the converter output voltage variation is very less so, the converter is not sensitive with change in coefficient value (k). Fig. 7 represents the graphical representation of the duty ratio versus output gain of the converter. In that, the x-axis is taken as duty ratio and the y-axis is taken as converter output voltage gain.

Table 3 represents the duty ratio versus voltage gain with coupling coefficient (k) is considered as 3 and varying CI values, the CI values are taken as 3, 4, 5, and 6. If the duty ratio is 0.9 with a CI value is 3 the converter produces 67 V, If the duty ratio is 0.9 with CI value is 4 the converter produces 86 V, If the duty ratio is 0.9

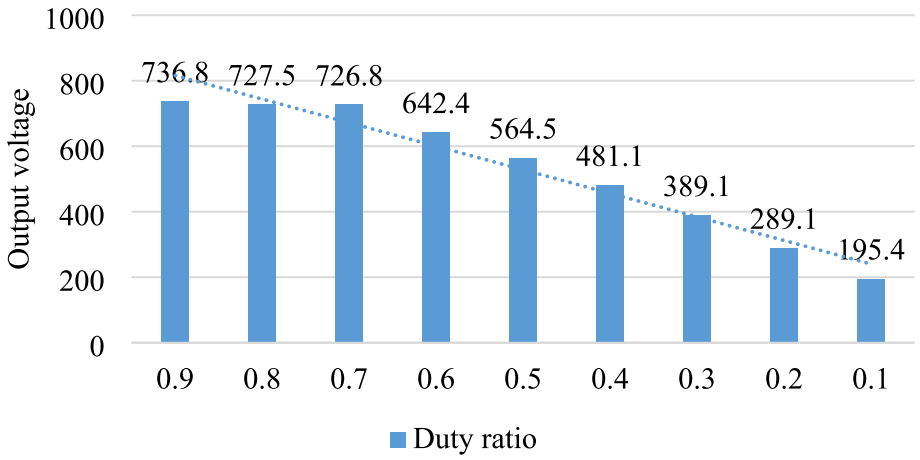

Fig. 6. Output voltage of the converter with a varying duty ratio from 0.1 to 0.9.

Table 1
Output voltage versus duty ratio.

Duty ratio	Output voltage (V)
0.9	736.8
0.8	727.5
0.7	726.8
0.6	642.4
0.5	564.5
0.4	481.1
0.3	389.1
0.2	289.1
0.1	195.4

Table 2
Duty ratio versus voltage gain.

Duty ratio	V_o/V_{in} under n = 3		
	K = 1	K = 0.98	K = 0.95
0.9	67.00	66.04	64.4
0.8	32.00	31.59	30.85
0.7	20.33	20.02	19.58
0.6	14.50	14.29	13.97
0.5	11.00	10.84	10.60
0.4	8.66	8.53	8.34
0.3	7.00	6.88	6.74
0.2	5.75	5.66	5.53
0.1	4.77	4.69	4.59

with CI value is 5 the converter produces 105 V, If the duty ratio is 0.9 with CI value is 6 the converter produce 124 V.

Table 3 can observe by changing the CI value the converter output voltage also changes. Fig. 8 represents the line diagram of duty ratio versus voltage gain, with different coupled inductor turns ratios (CI). Form Fig. 8 can be observed for more CI turns ratio produces more voltage gain.

4. Discontinuous conduction stage operation

In these three Stages are discussed.

$$V_{L1}^{1} = V_{in} \tag{15}$$

$$V_{L2}^{1} = nV_{in} \tag{16}$$

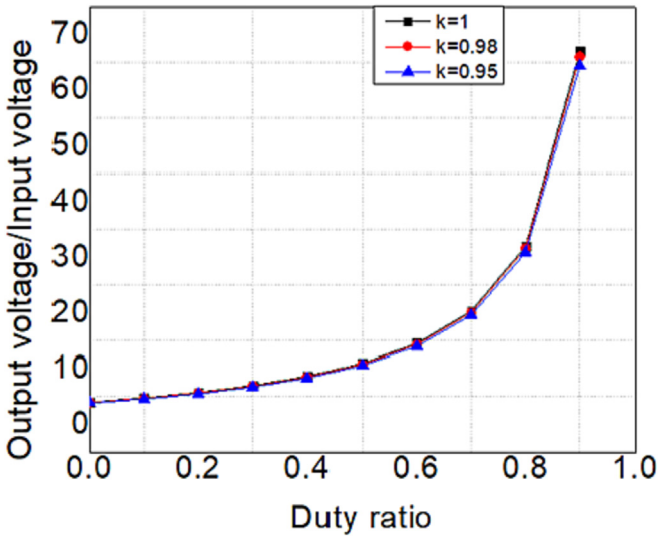

Fig. 7. Duty ratio versus voltage gain in CCS at n = 3 and different k's.

Table 3
Duty ratio versus CI turns ratio.

Duty ratio	V_o/V_{in} for k = 1			
	n = 3	n = 4	n = 5	n = 6
0.9	67.00	86.00	105.00	124.00
0.8	32.00	41.00	50.00	59.00
0.7	20.33	26.00	31.60	37.30
0.6	14.50	18.50	22.50	26.50
0.5	11.00	14.00	17.00	20.00
0.4	8.66	11.00	13.30	15.60
0.3	7.00	8.85	10.70	12.50
0.2	5.75	7.25	8.75	10.20
0.1	4.77	6.00	7.20	8.40

$$V_0 = V_{in} + V_{C1} + V_{C2} + V_{L2}^{1} + V_{C3} \tag{17}$$

For calculating the peak current of L_m is

$$I_{Lmp} = \frac{V_{in}}{L_m} DT_S \tag{18}$$

From Fig. 2 (Stage 2) the subsequence expression can be written (Stage-II)

$$V_{L1}^{2} = -V_{C1} \tag{19}$$

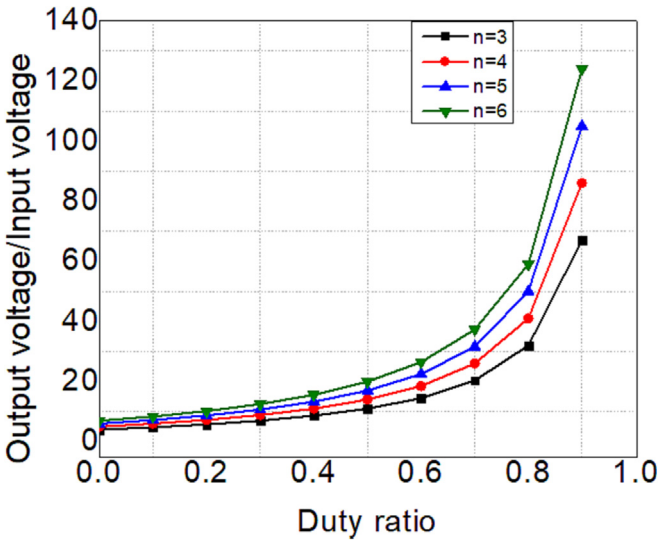

Fig. 8. Duty ratio versus voltage gain, with different coupled inductor turns ratio under k = 1.

$$V_{L2}^2 = -V_{C2} = -V_{C3} \tag{20}$$

From Fig. 2 (Stage 3) the subsequence expression can be written (Stage-III)

$$V_{L1}^3 = V_{L2}^3 = 0 \tag{21}$$

The subsequence expression can get from the coupled inductor by applying voltage balance principle

$$\int_0^{DT_S} V_{L1}^1 dt + \int_{DT_S}^{(D+D_L)T_S} V_{L1}^2 dt + \int_{(D+D_L)T_S}^{T_S} V_{L1}^3 dt = 0 \tag{22}$$

$$\int_0^{DT_S} V_{L2}^1 dt + \int_{DT_S}^{(D+D_L)T_S} V_{L2}^2 dt + \int_{(D+D_L)T_S}^{T_S} V_{L2}^3 dt = 0 \tag{23}$$

The capacitors voltages (C_1, C_2, and C_3) are got by substituting equations (15), 16, 18, 19 and 20 into equations (22) and (23)[28].

$$V_{C1} = \frac{D}{D_L} V_{in} \tag{24}$$

$$V_{C2} = V_{C3} = \frac{nD}{D_L} V_{in} \tag{25}$$

Voltage gain is got by substituting equations (16), 24 and 25 into equation (17)

$$V_0 = \left[\frac{D}{D_L}(2n+1) + (n+1)\right] V_{in} \tag{26}$$

D_L(Duty cycle) can be derived from equation (26)

$$D_L = \frac{(1+2n)DV_{in}}{V_0 - (1+n)V_{in}} \tag{27}$$

In a steady-state condition capacitor (C_2) releases its energy to R load and capacitor (C_0) Also, the average current

$$I_{D0} = I_{D2}$$

The average current of i_{CO} is

$$I_{C0} = I_{D0} = -I_0 = I_{D2} - I_0 = \frac{1}{2} D_L \frac{I_{Lmp}}{2n+1} - I_0 \tag{28}$$

In steady-state condition $I_{C0} = 0$, substituting equations (18) and (27) into equation (28)

$$\frac{D^2 V_{in}^2 T_S}{2[V_0 - (1+n)V_{in}]L_m} = \frac{V_0}{R} \tag{29}$$

$$T_{Lm} = \frac{L_m}{RT_S} = \frac{L_m f_S}{R} \tag{30}$$

Where, f_s = switching frequency.
Voltage gain can be got by insert equation (30) into 29

$$M_{DCS} = \frac{V_0}{V_{in}} = \frac{1+n}{2} + \sqrt{\frac{(1+n)^2}{4} + \frac{D^2}{2T_{Lm}}} \tag{31}$$

The voltage-gain of the modified converter in CCS and DCS are equal.

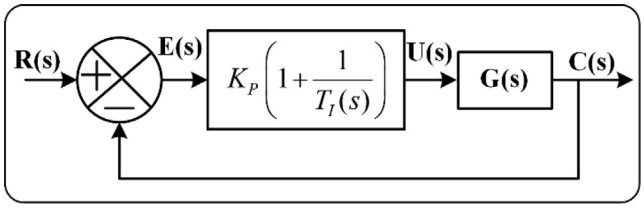

Fig. 9. PI controller block diagram.

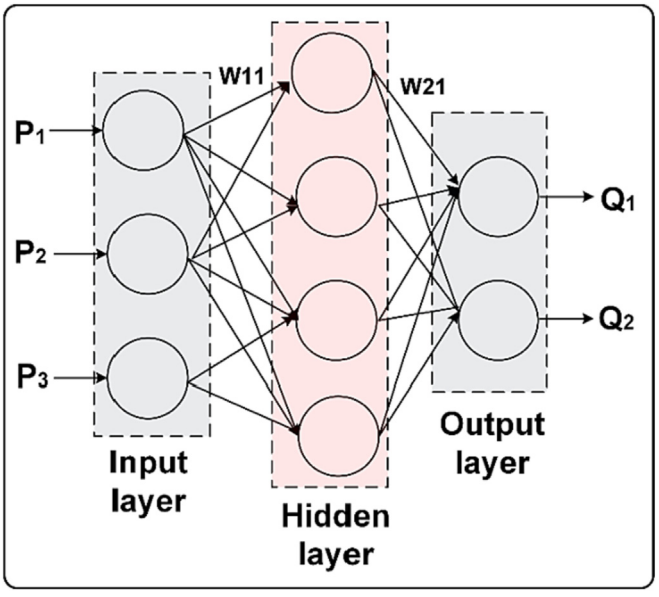

Fig. 10. Architecture of the neural network.

Table 4
Simulation specifications of the solar PV panel and converter.

Electrical Parameters	Values
Irradiance	200–1000 W/m^2
Open-circuit voltage (V_{oc})	23.88 V
Voltage at maximum power (V_{mp})	19.68 V
Short-circuit current (I_{sc})	9.6A
Current at maximum power (I_{mp})	9.15A
Maximum power at STC (Wp)	180Wp
DC input voltage (V_{in})	48 V
Clamp capacitor (C_1)	56uF/100 V
Charge Capacitors (C_2 and C_3)	22uF/200 V
Output capacitor (C_0)	180uF/450 V
DC Output voltage	400 V (nearly)

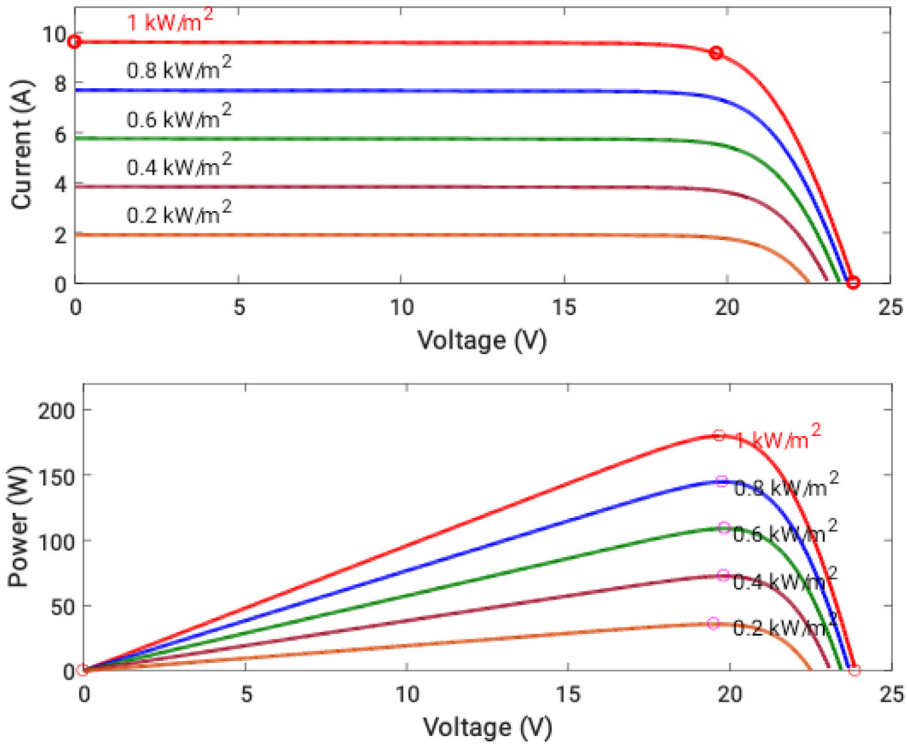

Fig. 11. I-V and P-V curves of the solar PV panel with various irradiance.

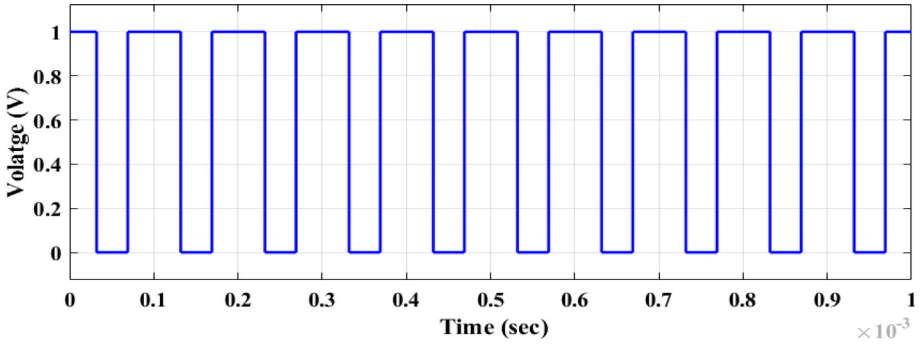

Fig. 13. Converter input and output voltages (a) with NN controller (b) with PI controller.

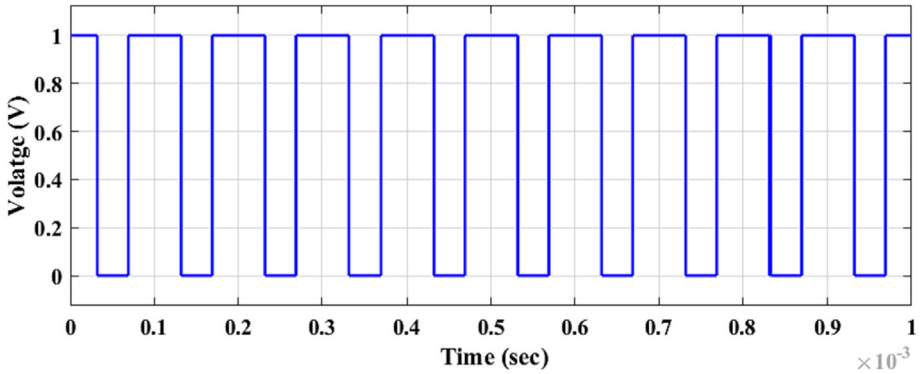

Fig. 12. Gate pulse of the converter switch.

5. Control techniques

5.1. Proportional integral

For reducing the steady-state error and increasing the system response Integral (I) controller was used but there is a disadvantage in the integral controller that is it will affect the stability of the system so to overcome this problem a Proportional Integral (PI) controller was introduced. This PI controller does the same work of the integral controller without affecting the stability of the system similarly reduce the steady-state error. The PI controller output must be proportional to an error signal and must be proportional to the integral of the error signal. Equation (32) represents the transfer function of the PI controller. By using the PI controller to decrease the steady-state error without disturbing

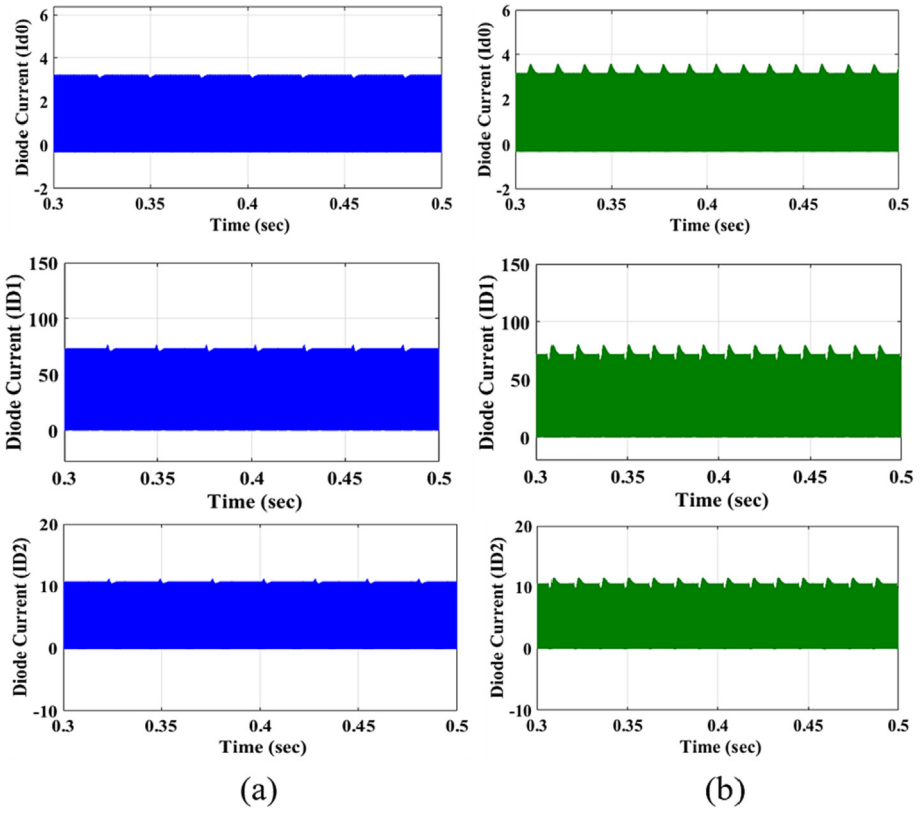

Fig. 14. Diodes currents of the modified converter (a) with the NN controller (b) with PI controller.

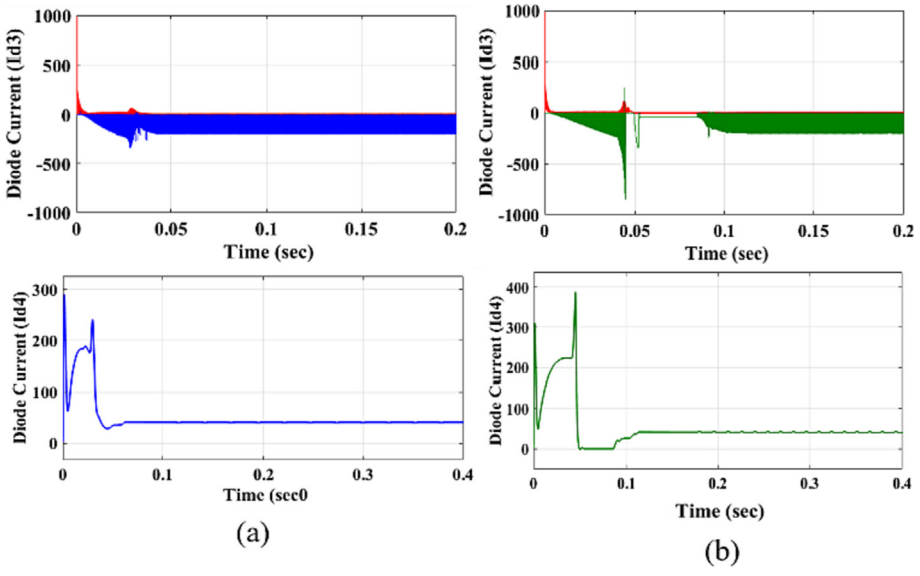

Fig. 15. Diode currents of the modified converter (a) with NN controller (b) with PI controller.

the stability of the system. The block diagram of the PI controller is shown in Fig. 9.[29]

$$G_C(s) = K_p\left(1 + \frac{1}{T_I S}\right) \quad \text{where} \quad T_I = \frac{K_P}{K_I} \tag{32}$$

By utilizing the PI controller to achieve accurate desired value, fast response and less error in steady-state.

5.2. Neural network

The NN has been used very effectively in the recognition and control of a dynamic system because of their universal approximation capability. NN controller has so many control algorithms that are presented based on the applications a specific algorithm is used. The P_1, P_2, and P_3 are the inputs of the controller similarly Q_1 and Q_2 are outputs of the controller. W_{11} and W_{22} indicate

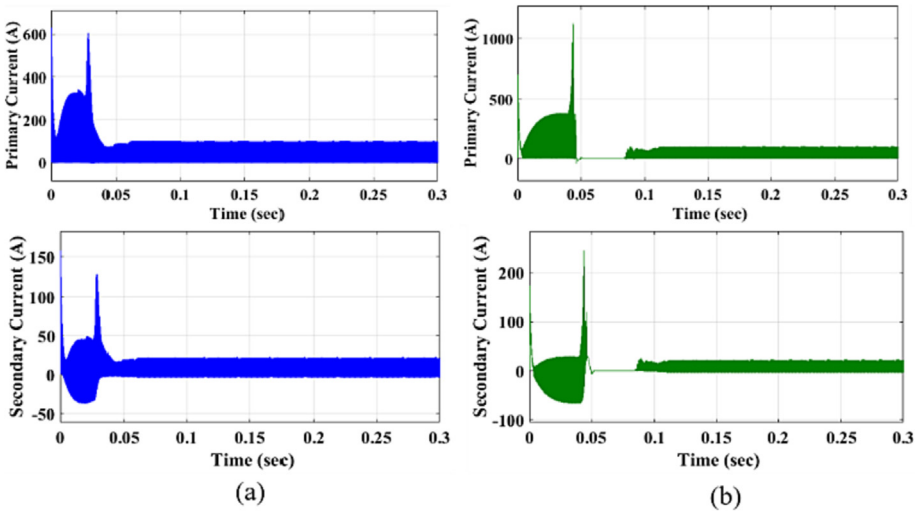

Fig. 16. CI primary and secondary currents of the modified converter (a) with NN controller (b) with PI controller.

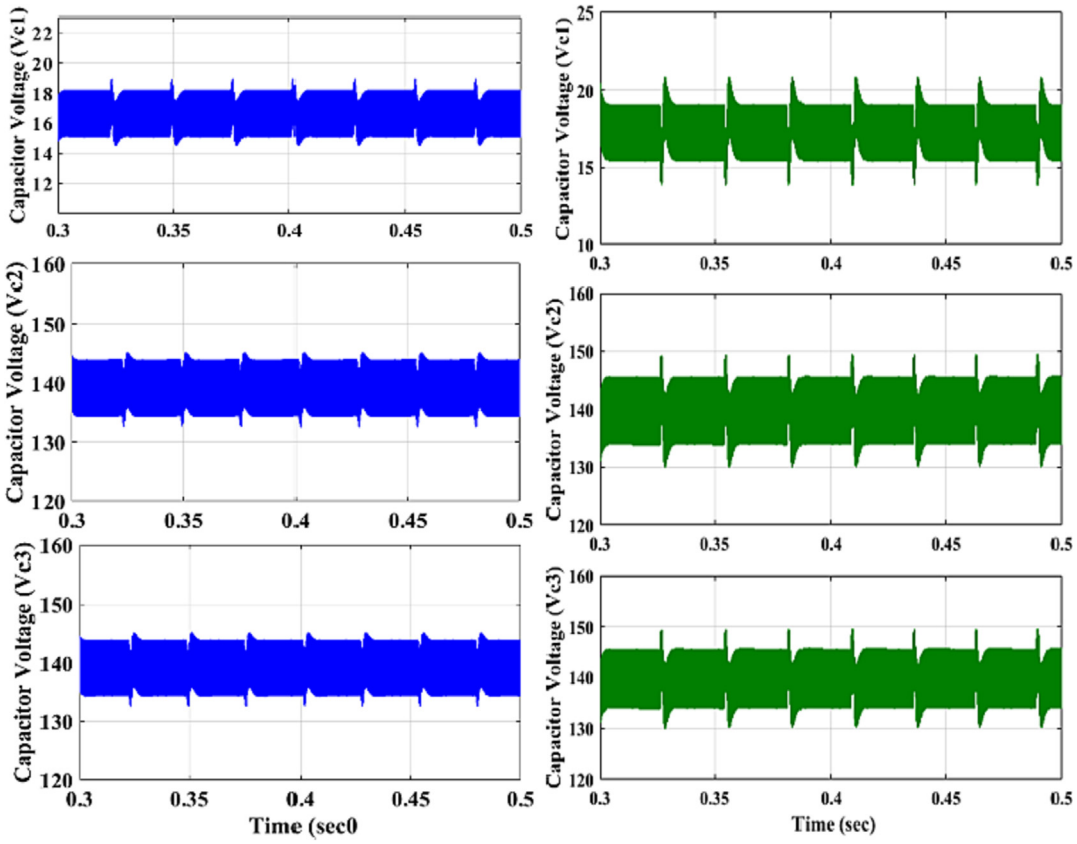

Fig. 17. Capacitor voltages of the modified converter (a) with NN controller (b) with PI controller.

the weight numbers if the connecting channels between the layers. In the NN controller mainly-three layers are present those are input layer, hidden layer, and output layer. Each layer is connected with proper weights. The NN controller was trained by a number of iterations and reduce the error then produce the appropriate signal to the plant. The block diagram of the NN controller is shown in Fig. 10.[30].

6. Simulation results

The input voltage of the converter is 48 V, it produces nearly 400 V as the output side of the converter. Table.4 represents the simulation specifications of the solar PV panel and converter. Here, the PI controller is used in a boost converter controlling. Here, PI and NN controllers are used in a boost converter controlling, Fig. 11 indicates the I-V and P-V curves of the solar PV panel with various irradiance, here the irradince range is taken form 200–1000 W/m^2. Fig. 12 indicates the gate pulse of the converter switch. The entire system was designed in MATLAB/ Simulink tool results are obtained Simulink/Matlab.

Fig. 13 indicates the input and output voltages of the modified converter, 13 (a) represent the NN controller-based converter outputs and 13 (b) represents the PI controlled based converter outputs. The NN controlled based converter has taken less settling time and fewer ripples on output voltages as compared to the PI controller-based converter.

Fig. 14indicate the diode (D_0, D_1, and D_2) currents of the modified converter, and Fig. 14 (a) represents the NN controller-based converter outputs andFig. 14 (b) represents the PI controlled based converter outputs. The NN controlled based converter have fewer ripples on output currents as compared to PI controller based converter.

Fig. 15 indicates the Diode (D_3 and D_4) input and output currents of the modified converter, Fig. 15 (a) represents the NN controller-based converter outputs and, Fig. 15 (b) represents the PI controlled based converter outputs. The NN controlled based converter have fewer ripples on diode currents as compared to PI controller based converter.

Fig. 16 indicates the CI primary and secondary currents of the modified converter, Fig. 16 (a) represents the NN controller-based converter outputs and, Fig. 16 (b) represents the PI controlled based converter outputs. The NN controlled based converter have fewer ripples on coupled inductor (CI) output currents as related to PI controller based converter.

Fig. 17 indicates the voltages of the capacitors of the modified converter, Fig. 17 (a) represents the NN controller-based converter outputs and Fig. 17 (b) represents the PI controlled based converter outputs. The NN controlled based converter have fewer ripples on output voltages as related to the PI controller based converter. These results were obtained from Simulink/MATLAB.

Table 5 represents the evaluation among the duty ratio versus voltage gain of the existing and proposed converters at n = 3 and k = 1. From Table.5 it shows that (Wai, R. J., et all, 2006 &Baek, J. W., et all, 2005), obtain the voltage gain of 37 V and 47 V respectively at the duty ratio of 0.9, whereas the converter produces a voltage gain of 67 V at the duty ratio of 0.9. Fig. 18 represents the duty ratio against the voltage gain of the proposed converter

Table 5
Evaluation among the duty ratio versus voltage gain of the existing and proposed converters.

Duty ratio	[24] Switchng mode	[25] Continous mode	Proposed
0.9	37.00	47.00	67.00
0.8	17.00	22.00	32.00
0.7	10.33	13.6	20.33
0.6	7.00	9.5	14.50
0.5	5.00	7.00	11.00
0.4	3.66	5.33	8.66
0.3	2.71	4.14	7.00
0.2	2.00	3.25	5.75
0.1	1.44	2.55	4.77

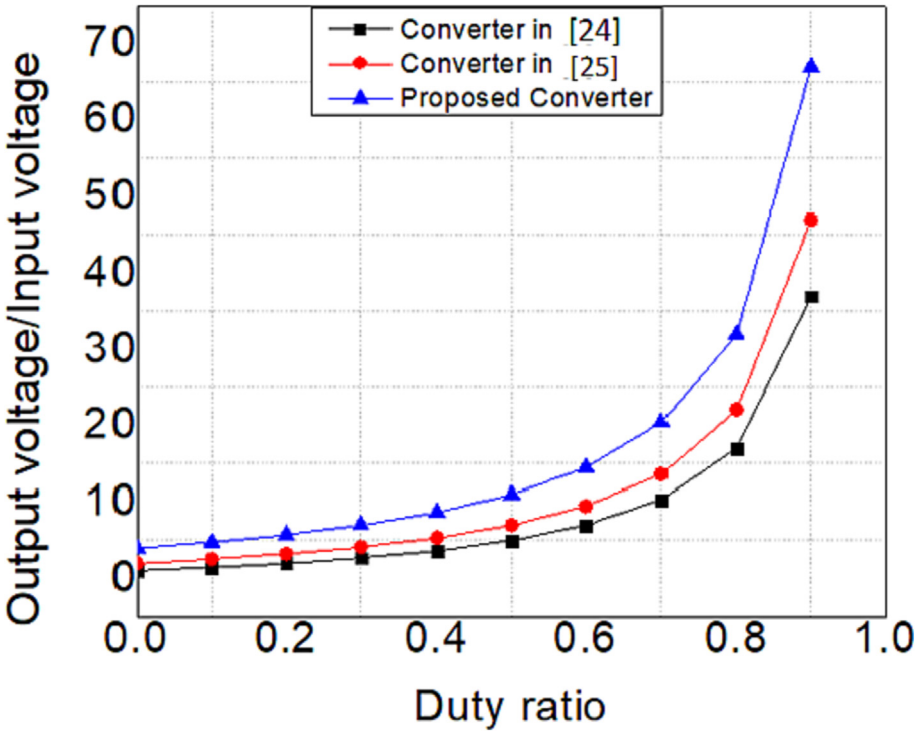

Fig. 18. Duty ratio versus voltage gain of the proposed converter versus existing converter at CCS at n = 3 and k = 1.

versus existing converters [24–25], at n = 3 and k = 1. The convert produces high voltage gain as compared to existing converters.

7. Conclusion

A modified high-voltage DC-DC converter has been explained for renewable energy applications. For achieving better efficiency and high-voltage, the capacitors are serially discharged and parallel charged through the coupled inductor. Mathematical modelling and converter analysis are explained in detail. In this, 48 V input is boosted up to 400 V nearly. By varying several parameters of the converter to observe the behaviour of the modified converter, similarly, observed the performance and behaviour of the modified converter versus existing converters. In this converter minimize the reverse recovery currents and voltage spicks across the switch. PI and NN controllers are used to control the switching pulse of the converter. The PI controller is unable to calculate the system future errors, so PI is unable to minimize settling time and oscillations in steady-state. Coming to NN, the settling time is fast and produces less oscillation in system output. So, finally by utilizing PI controller system stability is low as compared to the NN controller. Therefore Neural Network (NN) controller produces better system performance with minimum losses. In this converter minimize the reverse recovery currents and voltage spicks across the switch. PI and NN controllers are used to control the switching pulse of the converter The PI controller is unable to calculate the system future errors, so PI is unable to minimize settling time and oscillations in steady-state. Coming to NN, the settling time is fast and produces less oscillation in system output. So, finally by utilizing PI controller system stability is low as compared to the NN controller. Therefore Neural Network (NN) controller produces better system performance with minimum losses. Further the system can tune usng some optimizied algorthm for a better stability analysis.

Declaration of Competing Interest

The authors declare that they have no known competing financial interests or personal relationships that could have appeared to influence the work reported in this paper.

Acknowledgement

This work was supported in part by the Canada National Sciences and Engineering Research Council through the Laval University, Grant ALLRP567550-21.

References

[1] Lakshmi M, Hemamalini S. Coordinated control of MPPT and voltage regulation using single-stage high gain DC–DC converter in a grid-connected PV system. Electr Pow Syst Res 2019;169:65–73.
[2] Selim Aygen M, Inci Mustafa. Zero-sequence current injection based power flow control strategy for grid inverter interfaced renewable energy systems Energy Sources, Part A: Recovery. Utilization Environmental Effects 2022;44.
[3] El Mentaly L, Amghar A, Sahsah H. Comparison between Seven MPPT Techniques Implemented in a Buck Converter. Recent Advances in Electrical & Electronic Engineering (Formerly Recent Patents on Electrical & Electronic Engineering) 2019;12(6):476–86.
[4] Maity S, Varaprasad MVG. An efficient PV power optimizer with reduced EMI effects: Map-Based analysis and design technique. IEEE Trans Energy Convers 2017;33(2):546–55. doi: https://doi.org/10.1109/TEC.2017.2767629.
[5] MVG. Varaprasad, S. Maity, "Development of current sensorless photovoltaic mpp tracker." In *2019 International Conference on Computer, Electrical & Communication Engineering (ICCECE)*, pp. 1-5, Feb. 2020.DOI: 10.1109/ICCECE44727.2019.9001850.
[6] MVG. Varaprasad, S. Maity, "Microcontroller-Based Current Sensorless Photovoltaic MPP Tracker," In *2018 8th IEEE India International Conference on Power Electronics (IICPE)*, pp. 1-6, May. 2018.DOI:10.1109/IICPE.2018.8709496.
[7] Venkatesan R, Rajeshwari ND, Kaliyamoorthy M. Comparative study of three phase grid connected photovoltaic inverter using pi and fuzzy logic controller with switching losses calculation. Int J Power Electron Drive Syst 2016;7(2):543–50.
[8] Selim Aygen M, İnci M. Zero-sequence current injection based power flow control strategy for grid inverter interfaced renewable energy systems. Energy Sources Part A 2022;44(3):7782–803. doi: https://doi.org/10.1080/15567036.2020.1834029.
[9] Wai RJ, Duan RY. High-efficiency DC/DC converter with high voltage gain. IEE Proceedings-Electric Power Applications 2005;152(4):793–802. doi: https://doi.org/10.1049/ip-epa:20045067.
[10] Mustafa inci, Mehmet Selim Aygen. A modified energy management scheme to support phase balancing in grid interfaced photovoltaic/fuel cell system. Ain Shams Eng J 2021. doi: https://doi.org/10.1016/j.asej.2020.12.018.
[11] Tseng KC, Liang TJ. Novel high-efficiency step-up converter. IEE Proceedings-Electric Power Applications 2004;151(2):182–90. doi: https://doi.org/10.1049/ip-epa:20040022.
[12] Changchien SK, Liang T-J, Chen J-F, Yang L-S. Step-up DC-DC converter by coupled inductor and voltage-lift technique. IET Power Electron 2010.;3(3):369–78. doi: https://doi.org/10.1049/iet-pel.2009.0089.
[13] Axelrod YB, Ioinovici A. Switched-capacitor/switched-inductor structures for getting transformerless hybrid DC–DC PWM converters. IEEE Trans Circuits Syst I Regul Pap 2008;55(2):687–96. doi: https://doi.org/10.1109/TCSI.2008.916403.
[14] Li Y, Vilathgamuwa DM, Loh PC. Design, analysis, and real-time testing of a controller for multibusmicrogrid system. IEEE Trans Power Electron 2004;19(5):1195–204. doi: https://doi.org/10.1109/TPEL.2004.833456.
[15] Spiazzi G, Mattavelli P, Costabeber A. High step-up ratio flyback converter with active clamp and voltage multiplier. IEEE Trans Power Electron 2011;26(11):3205–14. doi: https://doi.org/10.1109/TPEL.2011.2134871.
[16] Luo FL, Ye H. Positive output cascade boost converters. IEE Proceedings-Electric Power Applications 2004;151(5):590–606. doi: https://doi.org/10.1049/ip-epa:20040511.
[17] Gules R, Dos Santos WM, Dos Reis FA, Romaneli EFR, Badin AA. A modified SEPIC converter with high static gain for renewable applications. IEEE Trans Power Electron 2013;29(11):5860–71. doi: https://doi.org/10.1109/TPEL.2013.2296053.
[18] Karimi H, Yazdani A, Iravani R. Negative-sequence current injection for fast islanding detection of a distributed resource unit. IEEE Trans Power Electron 2008;23(1):298–307. doi: https://doi.org/10.1109/TPEL.2007.911774.
[19] Shimizu KWd, Nakamura N. Flyback-type single-phase utility interactive inverter with power pulsation decoupling on the DC input for an AC photovoltaic modulesystem. IEEE Trans Power Electron 2006;21(5):1264–72. doi: https://doi.org/10.1109/TPEL.2006.880247.
[20] Zhao Q, Lee FC. High-efficiency, high step-up DC-DC converters. IEEE Trans Power Electron 2003;18(1):65–73. doi: https://doi.org/10.1109/TPEL.2002.807188.
[21] Yang LS, Liang TJ, Chen J-F. Transformerless DC–DC converters with high step-up voltage gain. IEEE Trans Ind Electron 2009.;56(8):3144–52. doi: https://doi.org/10.1109/TIE.2009.2022512.
[22] Wai RJ, Lin CY, Lin CY, Duan RY, Chang YR. High-efficiency power conversion system for kilowatt-level stand-alone generation unit with low input voltage. IEEE Trans Ind Electron 2008;55(10):3702–14. doi: https://doi.org/10.1109/TIE.2008.921251.
[23] Papanikolaou NP, Tatakis EC. Active voltage clamp in flyback converters operating in CCM mode under wide load variation. IEEE Trans Ind Electron 2004;51(3):632–40. doi: https://doi.org/10.1109/TIE.2004.825342.
[24] Abutbul O, Gherlitz A, Berkovich Y, Ioinovici A. Step-up switching-mode converter with high voltage gain using a switched-capacitor circuit. IEEE Transactions on Circuits and Systems I: Fundamental Theory and Applications 2003;50(8):1098–102. doi: https://doi.org/10.1109/TCSI.2003.815206.
[25] Dasari MS, Mani V. Simulation and analysis of PI and NN tuned PI controllers for transformer based three-phase multi-level inverter with MC-PWM techniques. Journal Européen des SystèmesAutomatisés 2019;52(6):587–98.
[26] Peniel Pauldoss S, Sekar K, Pattanaik B, Senthil Nayagam V. PV system with high voltage gain based DC-DC boost converter for grid applications. AIP Conf Proc 2022;2519:. doi: https://doi.org/10.1063/5.0110680050007.
[27] Mumtaz F, Yahaya NZ, Meraj ST, Singh B, Kannan R, Ibrahim O. Review on non-isolated DC-DC converters and their control techniques for renewable energy applications. Ain Shams Engineering JournalVolume 2021;12(4):3747–63. ISSN 2090–4479..
[28] Murillo-Yarce D, Restrepo C, Lamar DG, Sebastián J. A General Method to Study Multiple Discontinuous Conduction Modes in DC–DC Converters With One Transistor and Its Application to the Versatile Buck-Boost Converter. IEEE Trans Power Electron 2022;37(11):13030–46. doi: https://doi.org/10.1109/TPEL.2022.3187963.
[29] R. K. Pradhan and C. K. Sahu, "Single-input Fuzzy PI Controller for Traction Line-Side Converter of High Speed Railway," *2021 12th International Conference on Computing Communication and Networking Technologies (ICCCNT)*, 2021, pp. 1-6, doi: 10.1109/ICCCNT51525.2021.9579548.
[30] ChengYan, "A nural network indentification method for the inverter," 2008 International Conference on Electrical Machines and Systems, 2008, pp. 1810-1813.

Dasari Manikanta Swamy was born in Vizag, AP, India in 1994. He is currently associated with the Department of Electrical Engineering at Vignan's Institute of Information Technology, Vizag (Dt), India. He submitted his Ph.D. in the Department of Electrical Engineering at Vignan's Foundation for Science, Technology and Research University, Guntur, Andhra Pradesh, India. He received his B. Tech, in Electrical and Electronics Engineering from Vignan's Foundation for Science, Technology and Research University, Guntur, Andhra Pradesh, India, in 2015, and M. Tech. in Power Electronics and Drives from Vignan's Foundation for Science, Technology and Research University, Guntur, Andhra Pradesh, India. His current research interests include Power Electronics, DC-DC Converter, Multilevel Inverter, and Photovoltaic Based System Design.

Dr. Venkatesan Mani is currently associated with the Department of Electrical Engineering at Vignan's Lara Institute of Technology & Science, Guntur (Dt), India. He received his B.E., in Electronics and Communication Engineering from Anna University, Chennai, Tamil Nadu, India, M.E. in Power Electronics and Drives from Government College of Technology, Coimbatore, Tamil Nadu, India, and Ph.D. in Power Electronics from Anna University, Chennai, Tamil Nadu, India. His current research interests, include Power Electronics, DC-DC Converter, Multilevel Inverter, PV Based System Design. He is life Associate member of the Institution of Engineers (India).

Dr. Madisa V. G. Varaprasad received the B. Tech and M.Tech degrees in electrical and electronics engineering from the Vignan's Institute of Information Technology, Visakhapatnam, India, in 2011 and 2013, respectively. He completed his Ph. D. at the National Institute of Technology, Rourkela, India in 2020. Currently, he is working as an Assistant Professor in the Dept. of electrical and electronics engineering from the Vignan's Institute of Information Technology, Visakhapatnam, India. His research interest include modeling, analysis and control of photovoltaic, and power electronic converters systems.

Ramakrishna S S Nuvvula B.Tech degree in Electrical and Electronics from JNTU Kakinada 2012 and M.Tech from NITK .Phd from the VIT Vellore. Currently working in GMR Institute of Technology Rajam as an Assistant Professor

Md. Fatin Ishraque is from Rangpur, Bangladesh. He was born in Gaibandha, Bangladesh in 1997. He received the B.Sc. in Engineering degree in Electrical and Electronic Engineering (EEE) from Rajshahi University of Engineering & Technology in 2018. Currently he is pursuing his M.Sc. in Engineering Degree in Electrical and Electronic Engineering (EEE) from Rajshahi University of Engineering & Technology. At present, he is working a Lecturer in Dept of EECE in Pabna University of Science and Technology, Pabna, Bangladesh. His research interest includes Renewable energy, Dispatch strategy and IoT based system designing.

Dr. SK. A. SHEZAN is currently working as a lecturer in the Electrical Engineering department of the Engineering Institute of Technology, Melbourne, Australia and as a Research Fellow for School of Energy Engineering, Murdoch University, Perth, WA, Australia. He has been serving as a guest editor for Sustainability (MDPI) and the International Journal of Photoenergy (Hindawi). He completed his PhD degree in Electrical and Electronic Engineering from RMIT University, Melbourne, Australia. He was a lecturer in the Electrical and Electronics Engineering Department of Uttara University, Dhaka, Bangladesh. He received his Master of Engineering degree from the University of Malaya, in 2016. Moreover, he received his Bachelor of Engineering degree in Electrical Engineering and Automation from Shenyang University of Chemical Technology, China, in 2013. His research interests are Microgrid, HRES, Solar Energy, Wind Energy, Optimization, Power System Analysis, Energy Economics, etc.

Prof. Dr. Innocent Kamwa (Fellow, IEEE) received the Ph. D. degree in electrical engineering from Université Laval, in 1989. He was a Researcher at the Hydro-Québec's Research Institute, specializing in the dynamic performance and control of power systems. He was the Chief Scientist of Hydro-Québec's Smart Grid Innovation Program and an international consultant in power grid simulation and network stability. He is currently a Full Professor with the Department of Electrical Engineering and the Tier 1 Canada Research Chair in decentralized sustainable electricity grids for smart communities at Laval University. He is a fellow of the Canadian Academy of Engineering.

Prof. Dr. S. M. Muyeen (Senior Member, IEEE) received the B.Sc.Eng. degree in electrical and electronic engineering from the Rajshahi University of Engineering and Technology (RUET, formerly known as the Rajshahi Institute of Technology), Bangladesh, in 2000, and the M.Eng. and Ph.D. degrees in electrical and electronic engineering from the Kitami Institute of Technology, Japan, in 2005 and 2008, respectively. Currently, he is working as a Full Professor with the Electrical Engineering Department, Qatar University. He has been a keynote speaker and an invited speaker at many international conferences, workshops, and universities. He has published more than 250 articles in different journals and international conferences. He has published seven books as the author or an editor. His research interests include power system stability and control, electrical machine, FACTS, energy storage systems (ESSs), renewable energy, and HVDC systems. He is a fellow of Engineers Australia. He is serving as an Editor/Associate Editor for many prestigious Journals from IEEE, IET, and other publishers, including IEEE Transactions on Energy Conversion, IEEE Power Engineering Letters, IET Renewable Power Generation, and IET Generation, Transmission and Distribution.